



# Iodine doped carbon nanotube cables exceeding specific electrical conductivity of metals

Yao Zhao<sup>1\*</sup>, Jinquan Wei<sup>1,2\*</sup>, Robert Vajtai<sup>1</sup>, Pulickel M. Ajayan<sup>1</sup> & Enrique V. Barrera<sup>1</sup>

<sup>1</sup>Department of Mechanical Engineering and Materials Science, Rice University, Houston, United States, <sup>2</sup>Department of Mechanical Engineering, Tsinghua University, China.

Creating highly electrically conducting cables from macroscopic aggregates of carbon nanotubes, to replace metallic wires, is still a dream. Here we report the fabrication of iodine-doped, double-walled nanotube cables having electrical resistivity reaching  $\sim 10^{-7}$   $\Omega\cdot\text{m}$ . Due to the low density, their specific conductivity (conductivity/weight) is higher than copper and aluminum and is only just below that of the highest specific conductivity metal, sodium. The cables exhibit high current-carrying capacity of  $10^4\sim 10^5$  A/cm<sup>2</sup> and can be joined together into arbitrary length and diameter, without degradation of their electrical properties. The application of such nanotube cables is demonstrated by partly replacing metal wires in a household light bulb circuit. The conductivity variation as a function of temperature for the cables is five times smaller than that for copper. The high conductivity nanotube cables could find a range of applications, from low dimensional interconnects to transmission lines.

Since its discovery<sup>1</sup>, researchers have tried to translate the excellent properties of individual carbon nanotubes (CNTs) to larger assembled components. Among these, a macroscopic cable that would replace metals as a universal conductive wire would have large applicability<sup>2</sup>, such as electricity transmission, aerospace and automobile industry. Several methods have been developed for creating multi-walled, double-walled and single-walled carbon nanotube based fibers based on wet and dry spinning methods, over the years<sup>2-19</sup>. The main premise for these works has been to generate nanotube fibers with good mechanical properties. The electrical properties have also been reported with resistivities over a large range between  $7.1\cdot 10^{-3}$  to  $2\cdot 10^{-6}$   $\Omega\cdot\text{m}$ . In the supplementary information provided (Supplementary Table S1), we have listed and compared the resistivities of various nanotube fibers and metals prepared by a variety of techniques. For these fibers, up to now, their resistivity values are 2 to 3 orders higher than that for oxygen free Cu, ( $1.68\cdot 10^{-8}$   $\Omega\cdot\text{m}$ ), one of the most conducting metals widely used in current carrying applications.

## Results

Here we report the fabrication and doping of carbon nanotube cables (we have chosen to use the terminology “cable” rather than fiber, as the main application pursued here is electrical transport), with resistivity one order of magnitude closer to the resistivity of Cu than the predecessors. We believe that the superior conductivity is achieved by a synergistic effect of the unique structure of the CNTs, the rational design of processing and doping. Figure 1 (a) shows the nanotubes aligned in one direction, (see Methods and Supplementary Video S6 for processing information). Supplementary Figure S2 shows the nanotube bundles interconnected and formed into a continuous network (Macroscopically the continuous network has an open-ended cylindrical shape, which we call nanotube “stocking”). The small bundles and the nanotubes by themselves are several microns long. After the nanotubes were fabricated into the cable as shown in supplementary Fig. S2, the natural alignment of the nanotube “stocking” was retained which turns out to be beneficial for the conductivity of the cable. The nanotubes we have used here (Inset of Fig. 1b) are double-walled (DWNT); the diameters are in the range of 2–3 nm and uniform (Fig. 1b).

To improve the conductivity of the raw DWNT cable, the nanotubes were doped with iodine<sup>20-30</sup>. The raw DWNT cables were placed in the iodine vapor at 200°C for 12 hrs. Figure 1 (c) shows that the surface morphology of the iodine doped cable are similar to the raw cable. By SEM, we could not observe changes in diameter or any other morphology changes as a result of the iodine doping. Supplementary Figure S3 shows high contrast dark spots distributed over the surface of DWNTs, which could correspond to iodine clusters and atoms. The GIF

### SUBJECT AREAS:

CARBON NANOTUBES  
AND FULLERENES

ELECTRONIC MATERIALS AND  
DEVICES

NANOTECHNOLOGY  
MATERIALS SCIENCE

Received  
27 April 2011

Accepted  
15 August 2011

Published  
6 September 2011

Correspondence and  
requests for materials  
should be addressed to  
P.M.A. (ajayan@rice.  
edu) or E.V.B.  
(barrera@rice.edu).

\* These authors  
contributed equally to  
this work

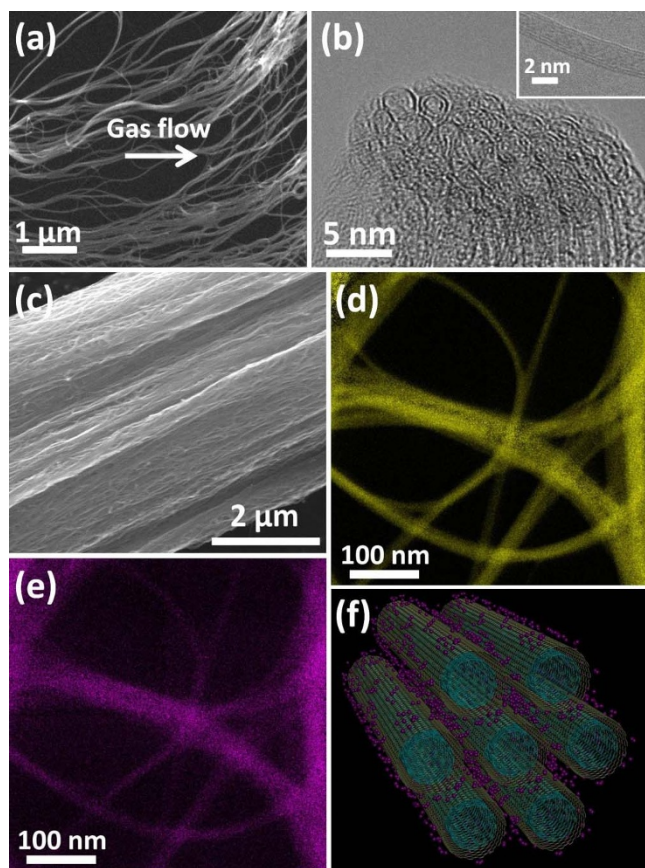


**Figure 1 | Morphology of the raw DWNTs and iodine doped DWNT cable, as well as composition of iodine doped DWNTs.** (a) SEM image of a small piece of the carbon nanotube film peeled off from the “stocking”. Carbon nanotubes are aligned in the gas flow direction as marked by the white arrow. (b) TEM image of a DWNT bundle tip. (c) SEM image of the iodine doped cable. Nanotubes are aligned in the long axis direction of the cable. (d) Elemental mapping of carbon by Gatan image filter (GIF). (e) Elemental mapping of iodine. (f) A schematic illustrating the speculated model for iodine doped nanotube bundle. The iodine atoms are decorating the surface of the nanotubes.

elemental mappings for carbon and iodine as shown in Fig. 1 (d) and Fig. 1 (e) indicate that the location of carbon and iodine overlap, suggesting that iodine is uniformly present within the cable. Figure 1 (f) is a schematic for the proposed model, where the iodine atoms are homogeneously adsorbed on the surface of DWNTs. The molecular simulation shows that iodine atoms are less likely to penetrate into the inter-layer spacing or inside of the tubes, especially when they are well capped. For the DWNT bundles, the iodine atoms can penetrate into interstitial spaces between tubes and form an intercalated structure. To reveal the bonding of iodine atoms with the DWNTs we observed their x-ray photoelectron spectra (XPS). The doped cable without any further treatment has an iodine atomic percentage of 3.3%. After washing and sonicating in ethanol, the iodine concentration drops to 2.1%. In an independent experiment, the doped cable was heated in vacuum ( $150^{\circ}\text{C}$  for 72hrs), which brought the iodine level to 2.3% (Fig. 2 (a)). These experiments show that the physically bonded iodine can be removed and the iodine remained on the surface of the DWNTs has a relatively strong chemical bonding. In comparison to the carbon XPS spectra before and after the doping (inset of Fig. 2(b) and Fig. 2(b), respectively), we can see the peak appearing at 285.2 eV after the doping, which corresponds to the energy of the C–I bonds. The peaks at 284.5 eV and 288.7 eV are assigned to C–C and C–O bonds, respectively. The C–O bonds are introduced during the purification procedure.

Resistivity of 34 raw DWNT cables with a diameter varying from  $4.1\ \mu\text{m}$  up to  $44.7\ \mu\text{m}$  was measured. Figure 3 (a) shows that statistically the cables of diameter  $>10\ \mu\text{m}$  have larger resistivity compared to cables of diameter  $<10\ \mu\text{m}$ . The size effect could be due to the fact that defects such as voids are invariably introduced into the larger cables during the fabrication process. The lowest resistivity found for the raw cables is  $\sim 5 \times 10^{-7}\ \Omega\cdot\text{m}$ . After doping with iodine, the cables further decreased in resistivity. The chemically bonded iodine as acceptors form  $(\text{I}_3)^-$  and  $(\text{I}_5)^-$  polyiodide chains in the intercalated sites, while mobile holes are created in the DWNTs. Due to the increasing density of mobile holes, the electrical conductivity of the cables was improved by the iodine doping<sup>21–22</sup>. X-ray diffraction spectra (Supplementary Fig. S4) shows that the (002) peak at  $2\theta \sim 10.86^{\circ}$  corresponding to the inter-layer spacing between the outer and inner wall of the DWNTs shifts to the higher angle after the iodine doping. The shift is due to the suppression of the inter-layer spacing from 3.76 Å to 3.63 Å. The X-ray spectra could be a direct

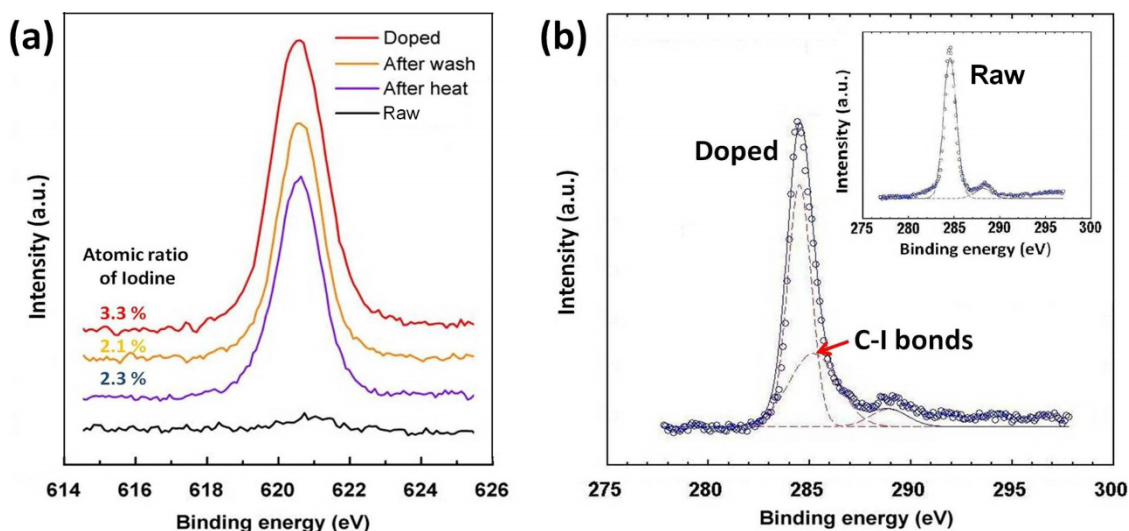


**Figure 2 | XPS spectra of the I-doped cable.** (a) Iodine spectra at different treatments. The black and red lines are the spectra for the cable before and after the iodine doping, respectively. The yellow line is collected from the doped cable after it was washed by ethanol. The blue line is collected from the doped cable after it was heated in the vacuum oven at  $150^{\circ}\text{C}$  for 72hrs. Inset of (b) and (b) are the XPS spectra for the cable before and after the iodine doping. The spectra curves (blue circles) are de-convoluted (dashed lines) by Gaussian fitting (solid lines), indicating multiple bonding energies.

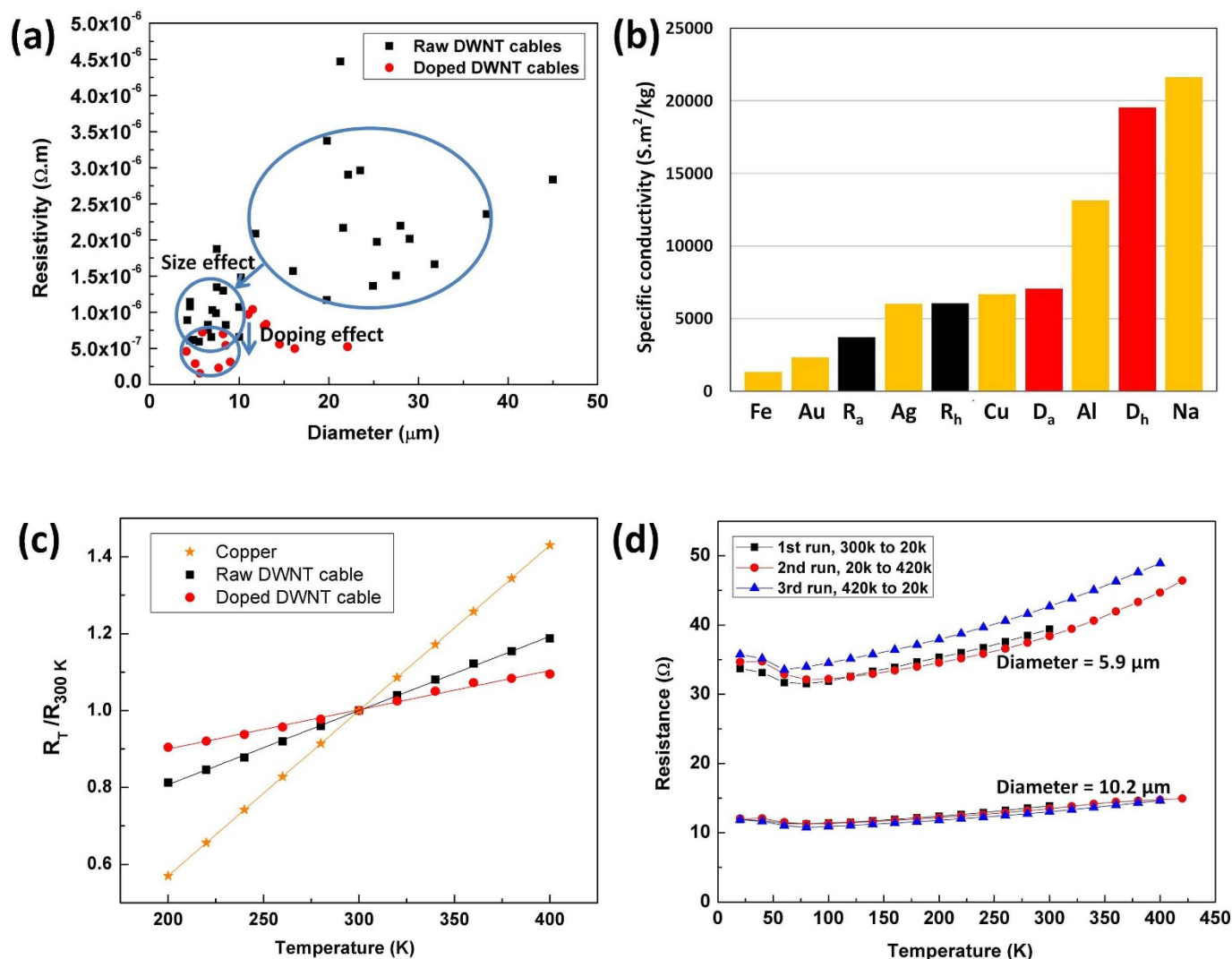


**Figure 3 | Electrical properties of the DWNT cables.** (a) The resistivity as a function of diameter for 34 raw DWNT cables and 15 iodine doped cables. (b) A comparison in specific conductivity among raw, doped cables and several metals.  $R_a$  and  $R_h$  represent for the average and the highest one for the raw cables.  $D_a$  and  $D_h$  are the values for the doped cables. (c) The relative resistance as a function of temperature for two doped cables. The thermal treatment for the cable of 10.2  $\mu m$  in diameter is continuous, but for the cable of 5.9  $\mu m$  in diameter, after the 2<sup>nd</sup> run of the heating process, the temperature was held at 420 k for 4 hrs, and then continued with the 3<sup>rd</sup> run.

indication of charge transfer and covalent bond formation. The lowest resistivity observed in our cables corresponds to  $\sim 1.5 \cdot 10^{-7} \Omega \cdot m$  for the doped cables. Although the raw DWNT cables are not as conductive as metals, their specific conductivity (conductivity/weight) value is very high as the density of the nanotube cable is much lower than the density of metals. The raw DWNT cables have an average density of 0.28  $g/cm^3$  and the iodine doped cables have an average density of 0.33  $g/cm^3$ . In terms of specific conductivity, the raw and doped cables are comparable with metals. For the iodine doped cables, the highest specific conductivity of  $1.96 \cdot 10^4 S \cdot m^2 / kg$  was observed, which is higher than that of Al and Cu, but slightly lower than that of sodium, which has the highest specific conductivity of among metals of  $2.16 \cdot 10^4 S \cdot m^2 / kg$ . A comparison in specific conductivity among raw, doped DWNT cables and a variety of metals is shown in Fig. 3 (b).

Copper is the most commonly used raw material for conducting wires. In this study, we compared the relative resistance (the ratio of the measured resistance,  $R_T$  to the resistance at 300 K,  $R_{300 K}$ ) of our cables with that of copper in the temperature range from 200 K to 400 K (normal operating temperature range for conducting wires). As shown in Fig. 3 (c), the reduced resistance versus temperature

curves for copper and the DWNT cables are both linear from 200 K to 400 K. For the iodine doped cable, the resistance at 200 K to 400 K varies by  $-9\%$  and  $9\%$  with respect to the resistance at 300 K. By contrast, the corresponding variations in copper are  $-43\%$  and  $43\%$ <sup>31</sup>. We also studied the stability of the electrical properties for the iodine doped cables. At room temperature, the doped cables kept the resistance value at a constant level for the whole testing period of a minimum seven days. Figure 3 (d) shows the resistance as a function of temperature measured on two of the doped cables. In the first experiment, a 10.2  $\mu m$  cable was continuously cooled down from room temperature to 20 K, heated up to 420 K, and cooled down to 20 K again. The heating/cooling rate was 1 K/min. The resistance versus temperature plot shows no hysteresis. This indicates that the iodine doping is stable upon the thermal cycling in this time scale.

Current carrying capacity is a property which measures the maximum current that can be passed through the unit cross sectional area of a conducting medium before it fails. An individual MWNT has extremely high current carrying capacity of  $10^9$ – $10^{10} A/cm^2$ <sup>32–33</sup>. This compares with nanoscale copper having a capacity of  $10^6 A/cm^2$ <sup>34</sup>. However, the current carrying capacity for the macroscopic nanotube cables as reported in literature is much



lower than that for individual single-walled nanotubes,  $10^5 \text{ A/cm}^2$ <sup>33</sup>. That finding is consistent with our results based on seven raw and seven iodine doped DWNT cables, which have current carrying capacities ranging from  $10^4$  to  $10^5 \text{ A/cm}^2$ . Although the macroscopic cables do not have the extremely high current carrying capacity of individual nanotubes, they still have a sufficiently high capacity to be capable of loading utilities even for small diameter cables. From W. H. Preece's formula, we calculated the current carrying capacity of the copper wires in open air to be  $10^4$  to  $10^5 \text{ A/cm}^2$  (The copper wires of diameter varying from  $5 \mu\text{m}$  to  $100 \mu\text{m}$ )<sup>35</sup>. DWNT cables' current carrying capacity is competitive to that of copper wires.

The nanotube cables also have the ability to be joined and assembled into larger structures. For example, two parallel DWNT cables were twisted and braided into one as shown in Fig. 4 (a). Before twisting, the two cables had resistances of  $24 \Omega$  and  $20 \Omega$  individually. Theoretically, the twisted thick cable from these two cables in a parallel configuration should have a resistance of  $10.9 \Omega$  ( $R_{\text{theoretical}} = 24 \Omega * 20 \Omega / (24 \Omega + 20 \Omega)$ ). From the measurement, we found that the assembled thick cable has a resistance of  $10.5 \Omega$ . This difference might be due to fact that the twisting renders better packing of the nanotubes in the cables and hence decreases the electrical resistivity of the individual cables themselves. This is a good indication suggesting that larger cable/wire structures of any arbitrary sizes can be built from the individual cables without sacrificing their electrical properties. Two individual cables (cable 1, diameter =  $13 \mu\text{m}$ ; cable 2, diameter =  $11.5 \mu\text{m}$ ) were also serially connected by a tie as shown in Fig. 4 (e). The two cables were knotted by a

micromanipulator. Traditional weaving techniques used in the textile industry should also be applicable for making such connections between cables. The resistivity of cable 1 and 2 individually are  $9.6 * 10^{-7} \Omega \cdot \text{m}$  and  $9.35 * 10^{-7} \Omega \cdot \text{m}$ , respectively. Based on the resistivity, diameter and length of each cable (length is for the segment between the tie and its adjacent electrode), we can calculate the resistance of cable 1 and 2 as  $15.33 \Omega$  and  $16.34 \Omega$ . The assembled structure of cable 1, cable 2 and the tie has a resistance of  $31.9 \Omega$ . The resistance from the tie would then be  $\sim 0.23 \Omega$  suggesting that no significant resistance is introduced by the knot and indeed several short cables could be easily assembled to longer ones. The cable as the conducting wire is demonstrated in a circuit as shown in Fig. 4 (b) and (d). A household bulb (9 watts, 0.15A, 120V) was connected with the public power supply through the twisted wire. The light bulb was powered up. The circuit was turned on for 3 days. The nanotube cable functioned well for the whole testing period. In the circuit, the cable replaced a section of copper wire as shown in Fig. 4 (c). Here the nanotube cable is much smaller in diameter than copper wires. It is also found that the cables are mechanically quite robust. The average ultimate tensile strengths for the undoped and doped cables are  $320 \text{ MPa}$  and  $640 \text{ MPa}$ , respectively, comparable to metals. Supplementary Figure S5 shows the stress-strain curves for the two samples; after doping, the cable's strength increased but the strain to failure became smaller.

## Discussion

In summary, we have made double-walled carbon nanotube cables that outperform Cu and Al in specific electrical conductivity. Iodine doping effectively increases the conductivity of the cables, as well as their tensile strength. Using cables as the building blocks and employing different assembly methods, larger and longer wires and cables can be created and we have used this approach to demonstrate a nanotube wire circuit to power a household light bulb. These lightweight nanotube cables could be serious contenders for replacing metal wires in electrical transmission as they would have intrinsic advantages to metals such as high temperature stability and chemical resistance.

## Methods

The cable preparation includes four steps: nanotube growth, nanotube purification, soaking in the sulfuric acid and shrinking.

**Nanotube growth.** Double-walled carbon nanotubes (DWNTs) were grown by flow chemical vapor deposition (CVD) method (See Supplementary Video S6)<sup>36–37</sup>.

**Nanotube purification.** The DWNTs as-grown contain catalysts. It was found that impurities cause degradation in conductivity. Therefore, we purified DWNTs before making them into cables. The DWNTs were first oxidized by heating the raw macroscopic DWNT bundle in air at  $400^\circ\text{C}$  for 1 hour. The oxidation treatment can attach oxidized functional groups to nanotubes and make DWNTs be of a better wettability with water. Then the oxidized DWNTs were soaked into a 30% hydrogen peroxide solution for 72 hours. This soaking process can crack the amorphous carbon and make the catalysts dissociate from the carbon nanotubes. Afterward, the DWNTs were transferred into a 37% hydrogen chloride solution and soaked for another 24 hours. Then, the DWNTs as received from the previous procedure were washed by DI water until they become neutralized<sup>38</sup>. After the purification, the catalyst weight percentage is below 1%.

**Soaking in the sulfuric acid.** The diameter of cables is determined by how much DWNTs would be used to make the cable. The purified DWNTs in water are in a bundled form because of van der Waals interaction between tubes. The big bundle would result in making a cable of diameter larger than  $20 \mu\text{m}$ . To peel off a small amount of DWNTs from the bundle to make a cable of diameter sub- $10 \mu\text{m}$ , the bundle needs to be spread. The DWNT bundle was loosened up and spread into thin films by soaking in 98% sulfuric acid for 24 hours. After the soaking treatment, the DWNTs have a form as shown in Supplementary Fig. S7. From the thin film, a small amount of DWNTs in a ribbon form can be peeled off.

**Shrinking.** When the DWNT ribbon was taken out from the sulfuric acid solution, it would agglomerate into a spherical particle because the surface tension caused by the residual sulfuric acid is isotropic. To retain the length in the long axis direction of the ribbon, we applied the pulling force on the two ends of the ribbon to counteract

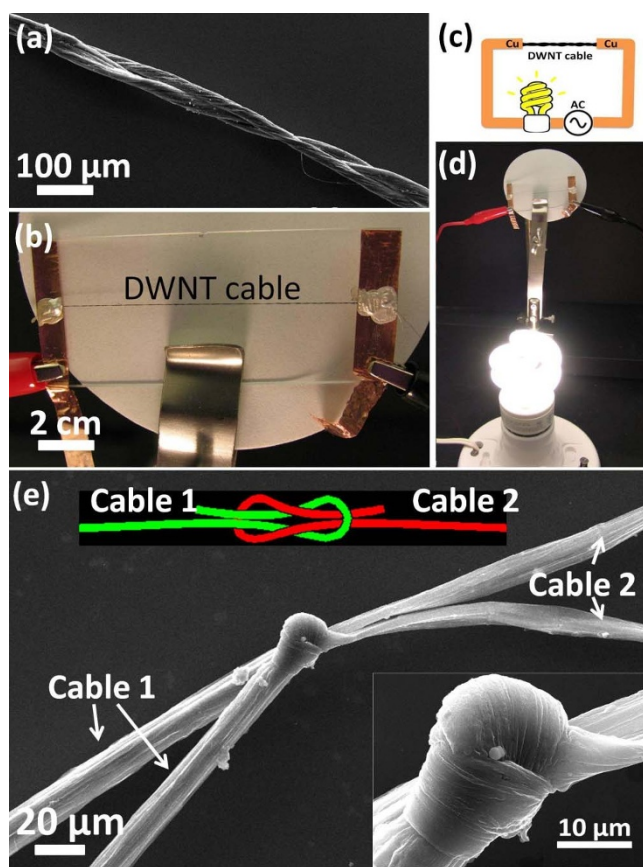


**Figure 4** | DWNT cables used in parallel and series electrical circuits. (a) SEM image of two cables twisted in a parallel configuration. (b) The image of the twisted cable. (c) Schematics of the circuit (d) The cable as a segment of conductive media connected with the household power supply and loaded with a light bulb (9 watts, 0.15 A, 120 V). (e) SEM images shows that cable 1 and 2 can be knotted and joined. Inset is a higher magnification SEM image of the tie.



the tension force from the sulfuric acid when the ribbon was taken out of the sulfuric acid solution. Then, the ribbon was dipped into the DI water to wash out the residual acid. Afterward, the ribbon was taken out of the water. Along with the water evaporation process, the ribbon shrunk into the cables. The shrinking was a synergistic effect of the van der Waals force between tubes and the surface tension force from the water. At the last step of shrinking, other solutions such as ethanol, acetone and chloroform can be the substitutions for water. Microscopically, the original loose DWNT networks shrunk into a dense form.

After the raw cables were prepared, the iodine doping was conducted by placing the raw DWNT cables in the iodine vapor (the iodine vapor concentration is 0.2 mol/l) at 200°C for 12 hrs.

**Structure and composition analysis.** Transmission electron microscopy (TEM) was applied to observe nanostructures of DWNTs and iodine doped DWNTs. Scanning electron microscopy (SEM) was used to measure the diameter of cables and to observe the structure and the morphology of DWNTs before and after each step of the processing. The elemental composition of the iodine doped cables was characterized by x-ray photoelectron spectroscopy (XPS). To understand the distribution of iodine atoms, the elemental mapping for the iodine doped DWNTs was obtained via a Gatan imaging filter (GIF) attached with the TEM. In addition, Polarized Raman spectra of the raw and iodine doped cables were collected for both the parallel and perpendicular directions to the long axis of the cables (See Supplementary Fig. S8). For this study, a 632 nm laser associated with an 1800/m grating were used. X-ray diffraction spectra were collected for both the raw and iodine doped DWNTs. The X-ray source was generated from a Mo target.

**Electrical property measurements.** Resistivity was calculated based on the length  $L$ , diameter  $D$  and resistance  $R$  of the cables using the formula,  $\text{resistivity} = R \cdot D^2 \cdot \pi / 4L$ . The calculation is based on the assumption that cables are in a cylindrical shape. In fact, the cross section of some cables is not an ideal circle but an ellipse. In the calculation, we used long axis length as the diameter. By this approximation, the real resistivity of the cable is lower than the calculated value. Diameter,  $D$  of each cable plugged into the formula was an average based on the measurements at three different locations along the cable's long axis direction. The data reported in this study was based on the cables with a diameter variation smaller than 10% along the cable's long axis direction. The resistance was characterized by a Keithley 2400 in a four-probe configuration. The representative I-V curve for reading the resistance of the cable was shown in Supplementary Fig. S9.

Current carrying capacity was defined by the ratio of the critical current to the cross sectional area. The cable was connected with a Keithley 2400, which was the current source by two electrodes. The current passing the cable was stepwise increased. The critical current was recorded at the moment that the cable was burned. The representative current versus time curve for recording the critical current was shown in Supplementary Fig. S10.

**Mechanical property measurements.** Tensile test was conducted on five undoped and five doped cables using an electrodynamic test system (Electroplus 3000, Instron). The strain rate was set at 0.2%/S.

- Iijima, S. Helical microtubules of graphitic carbon. *Nature* **354**, 56-58 (1991).
- Ericson, L. M. *et al.* Macroscopic, neat, single-walled carbon nanotube fibers. *Science* **305**, 1447-1450 (2004).
- Vigolo, B. *et al.* Macroscopic fiber and ribbons of oriented carbon nanotubes. *Science* **290**, 1331-1334 (2000).
- Dalton, A. B. Super-tough carbon-nanotube fibres. *Nature* **423**, 703 (2003).
- Zhang, M., Atkinson, K. R. & Baughman, R. H. Multifunctional carbon nanotube yarns by downsizing an ancient technology. *Science* **306**, 1358-1361 (2004).
- Motta, M., Li, Y., Kinloch, I. A. & Windle, A. H. Mechanical properties of continuously spun fibers of carbon nanotubes. *Nano Letters* **5** (8), 1529-1533 (2005).
- Annamalai, R., West, J. D., Luscher, A. & Subramaniam, V. V. Electrophoretic drawing of continuous fibers of single-walled carbon nanotubes. *J. Appl. Phys.* **98**, 114307 (2005).
- Koziol, K. *et al.* High-performance carbon nanotube fiber. *Science* **318**, 1892-1895 (2007).
- Zhang, X. F. *et al.* Ultrastrong, stiff and lightweight carbon-nanotube fibers. *Adv. Mater.* **19**, 4198-4201 (2007).
- Chae, H. & Kumar, S. Making strong fibers. *Science* **319**, 908-909 (2008).
- Davis, V. A. *et al.* True solutions of single-walled carbon nanotubes for assembly into macroscopic materials. *Nature nanotechnology* **4**, 830-834 (2009).
- Naraghi, M. *et al.* A multiscale study of high performance double-walled nanotube-polymer fibers. *ACS Nano* **4** (11), 6463-6476 (2010).
- Badaire, S. Correlation of properties with preferred orientation in coagulated and stretch-aligned single-wall carbon nanotubes. *J. Appl. Phys.* **96** (12), 7509-7513 (2004).
- Steinmetz, J., Glerup, M., Paillet, M., Bernier, P. & Holzinger, M. Production of pure nanotube fibers using a modified wet-spinning method. *Carbon* **43**, 2397-2399 (2005).

- Kozlov, M. E. *et al.* Spinning solid and hollow polymer free carbon nanotube fibers. *Adv. Mater.* **17** (5), 614-617 (2005).
- Jang, E. Y. *et al.* Macroscopic single-walled-carbon-nanotube fiber self-assembled by dip-coating method. *Adv. Mater.* **21**, 4357-4361 (2009).
- Zhang, X. F. *et al.* Strong carbon-nanotube fibers spun from long carbon-nanotube arrays. *Small* **3** (2), 244-248 (2007).
- Liu, K. *et al.* Scratch-resistant, highly conductive, and high-strength carbon nanotube based composite yarns. *ACS nano* **4** (10), 5827-5834 (2010).
- Zhong, X. H. *et al.* Continuous multilayered carbon nanotube yarns. *Adv. Mater.* **22**, 692-696 (2010).
- Lee, R. S., Kim, H. J., Fischer, J. E., Thess, A. & Smalley, R. E. Conductivity enhancement in K- and Br- doped nanotube bundles. *Nature* **388**, 255-257 (1997).
- Grigorian, L. *et al.* Reversible intercalation of charged iodine chains into carbon nanotube ropes. *Phys. Rev. Letts.* **80** (25), 5560-5563 (1998).
- Fischer, J. E. Chemical doping of single-walled carbon nanotubes. *Acc. Chem. Res.* **35**, 1079-1086 (2002).
- Niyogi, S. *et al.* Chemistry of single-walled carbon nanotubes. *Acc. Chem. Res.* **35**, 1105-1113 (2002).
- Kumari, L., Prasad, V. & Subramanyam, S. V. Effect of iodine incorporation on the electrical properties of amorphous conducting carbon films. *Carbon* **41**, 1841-1846 (2003).
- Cambedouzo, J. *et al.* Raman spectroscopy of iodine-doped double-walled carbon nanotubes. *Phys. Rev. B* **69**, 235422 (2004).
- Kissell, K. R., Hartman, K. B., Van der Heide, P. A. W. & Wilson, L. J. Preparation of I<sub>2</sub>@SWNTs: synthesis and spectroscopic characterization of I<sub>2</sub>-loaded SWNTs. *J. Phys. Chem. B* **110**, 17425-17429 (2006).
- Michel, T. *et al.* Structural selective charge transfer in iodine-doped carbon nanotubes. *J. Phys. Chem. Solids* **67**, 1190-1192 (2006).
- Khoerunnisa, F. *et al.* Electronically modified single wall carbon nanotubes with iodine adsorption. *Chem. Phys. Letts.* **501**, 485-490 (2011).
- Zhou, W. Y. *et al.* Raman scattering and thermogravimetric analysis of iodine-doped multiwall carbon nanotubes. *Appl. Phys. Lett.* **80** (14), 2553-2555 (2002).
- Choi, W. I., Ihm, J. & Kim, G. Modification of the electronic structure in a carbon nanotube with the charge dopant encapsulation. *Appl. Phys. Lett.* **92**, 193110 (2008).
- Copper wire tables. *National Bureau of Standards Handbook 100* (U.S. government printing office, Washington D.C., Issued Feb. 21 1966).
- Wei, B. Q., Vajtai, R. & Ajayan, P. M. Reliability and current carrying capacity of carbon nanotubes. *Appl. Phys. Lett.* **79** (8), 1172-1174 (2001).
- Ma, J., Tang, J., Zhang, H., Shinya, N. & Qin, L. C. Ultrathin carbon nanotube fibrils of high electrochemical capacitance. *ACS nano* **3** (11), 3679-3683 (2009).
- Murali, R., Yang, Y. X., Brenner, K., Beck, T. & Meindl, J. D. Breakdown current density of graphene nanoribbons. *Appl. Phys. Lett.* **94**, 243114 (2009).
- Preece, W. H. *Royal Soc. Proc.* **36**, 464 (1884).
- Wei, J. Q. *et al.* Preparation of highly pure double-walled carbon nanotubes. *J. Mater. Chem.* **13** (6), 1340-1344 (2003).
- Ci, L. J. *et al.* Double wall carbon nanotubes promoted by sulfur in a floating iron catalyst CVD system. *Chem. Phys. Letts.* **359**, 63-67 (2002).
- Wang, Y. H., Shan, H. W., Hauge, R. H., Pasquali, M. & Smalley, R. E. A highly selective, one-pot purification method for single-walled carbon nanotubes. *J. Phys. Chem. B* **111**, 1249-1252 (2007).

## Acknowledgments

The authors gratefully acknowledge financial support for this research from the Research Partnership to Secure Energy of America (RPSEA), the United States Department of Energy (grant No. D-74876) and AFRL (grant No. FA 8650-08-2-5061). We are also grateful to Zheng Liu, Pdraig Monoley, James Huang (Boeing Research & Technology, Huntington Beach, CA), Andres Rodela and Fangbo Xu for helpful discussion.

## Author contributions

Y. Z and J.Q.W. contributed equally to this work. Y.Z. and J.Q.W. designed and carried out the experiments (CVD, SEM, TEM, XPS, Raman, fiber preparation, electrical test), and analyzed the data. P.M.A. and E.V.B. was responsible for the project planning. Y.Z., J.Q.W., R.V., P.M.A. and E.V.B. co-wrote the paper. All the authors discussed the results.

## Additional information

**Supplementary information** accompanies this paper at <http://www.nature.com/scientificreports>

**Competing financial interests:** The authors declare no competing financial interests.

**License:** This work is licensed under a Creative Commons Attribution-NonCommercial-ShareAlike 3.0 Unported License. To view a copy of this license, visit <http://creativecommons.org/licenses/by-nc-sa/3.0/>

**How to cite this article:** Zhao, Y., Wei, J., Vajtai, R., Ajayan, P.M. & Barrera, E.V. Iodine doped carbon nanotube cables exceeding specific electrical conductivity of metals. *Sci. Rep.* **1**, 83; DOI:10.1038/srep00083 (2011).